VOL. 13, NO. 24, DECEMBER 2018 ISSN 1819-6608
ARPN Journal of Engineering and Applied Sciences

www.arpnjournals.com

# INDIRECT MEASUREMENT OF FREE-STREAM TURBULENCE LEVEL IN WIND TUNNELS

Ercan Erturk[1] and Orhan Gokcol[2]
[1]Bahcesehir University, Mechatronics Engineering Department, Besiktas, Istanbul, Turkey
[2]Bahcesehir University, Computer Education and Instructional Technologies Department, Besiktas, Istanbul, Turkey
E-Mail: ercan.erturk@eng.bau.edu.tr

## ABSTRACT

In this study we investigate the possibility of predicting the free stream turbulence levels by an indirect measurement. The main motivation for this is that in some wind tunnels direct hot wire measurements are not possible and there is a need to measure the turbulence levels in these wind tunnels. We constructed a flat-plate model with a 6:1 ellipse as a leading edge and place it inside a wind tunnel. Inside the wind tunnel the turbulence was produced by one of three different perforated grids, with different holes and mesh sizes. The free-stream turbulence conditions were documented for the three grids in terms of the total r.m.s. and spectra of stream wise velocity fluctuations. The response of the boundary layer near the leading edge was then measured through wall-normal profiles of the mean and r.m.s. velocity fluctuations. We find a linear input-output response of the Klebanoff mode amplitude with the free-stream turbulence level.

**Keywords:** wind tunnel, indirect free-stream turbulence measurement.

## 1. INTRODUCTION

In this study we try to development of a method for the indirect measurement of free-stream turbulence levels which are suitable for adverse conditions that exist in cryogenic wind tunnels. The approach is based on measuring the amplitude of Klebanoff modes [1] which are known to develop through the interaction of turbulent scales and a leading edge. The advantages of this approach are that these modes occur at low frequencies and therefore do not require high frequency response (delicate) sensors, that their amplitudes vary linearly with free-stream amplitude, and that their amplitude grows as the square-root of the distance from the leading edge, making it possible to have a relatively short model. Furthermore, it is known that the most amplified Klebanoff mode [1] is not sensitive to its span-wise wave length so that the span-wise spacing of sensors can be determined a priori. Finally these modes are probably not sensitive to the level of acoustic disturbances so that they will directly reflect the level of vortical fluctuations in the tunnel. To investigate this, we constructed a flat-plate model with a 6:1 ellipse as a leading edge. This was placed in a wind tunnel with different intensities and scales of turbulence. The turbulence was produced by one of three different perforated grids, with different holes and mesh sizes. These were carefully selected so that combinations of turbulence intensities and scales could be independently changed. The free-stream turbulence conditions were documented for the three grids in terms of the total r.m.s, and spectra of stream wise velocity fluctuations. The response of the boundary layer near the leading edge was then measured through wall-normal profiles of the mean and r.m.s. velocity fluctuations.

## 2. EXPERIMANTEL SETUP

A flat plate with a 6:1 elliptic leading edge was manufactured and it was placed inside the test section of a wind tunnel. The 6:1 ratio in the leading edge was selected in order to match the experimental setup of Kendall (1985, 1990) [2,3]. In order to produce different turbulence levels and scales in the flow, different perforated grids were used. These perforated grids were placed at the entrance of the test section upstream of the flat plate with a 6:1 elliptic leading edge. The schematic and the characteristics of the perforated grids used are given in Figure-1 and Table-1 respectively. In this study 3 different perforated plate with different hole diameters and mesh were used. These 3 different perforated grids were designated as PP (perforated plate) numbers 1,2 and 3. The perforated grids used in this study were chosen as identical with the perforated grids used in Loehrke and Nagib (1972) [4], with the same designation. Their [4] data was useful for predicting the rate of turbulence decay downstream of the grids, and the closest location where a uniform mean flow could be expected.

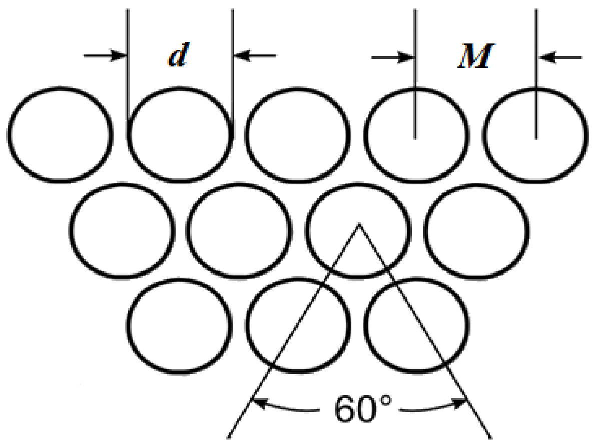


**Figure-1.** Schematic view of the perforated grids.

VOL. 13, NO. 24, DECEMBER 2018 ISSN 1819-6608
ARPN Journal of Engineering and Applied Sciences


www.arpnjournals.com

**Table-1.** Characteristics of perforated grids used for controlling free-stream turbulence levels.

| Designation | Hole diameter ($d$)(cm) | Mesh ($M$) (cm) | Solidity ($\sigma$)(%) |
|---|---|---|---|
| PP#1 | 0.16 | 0.28 | 0.70 |
| PP#2 | 0.36 | 0.48 | 0.49 |
| PP#3 | 0.64 | 0.80 | 0.42 |

The flat plate was built as a composite structure by bonding 16 gauge (0.152cm thick), 430 series stainless steel sheets to either side of a 45.7cm wide by 121.9cmlong, by 1.9cm thick particle board. The 430 alloy has high chrome content so that the cold-rolled sheet has an extremely smooth, highly polished finish.

The elliptic leading edge was machined separately and attached to the upstream end of the flat plate. The surface was filled to eliminate any surface imperfections, and polished smooth. The joint with the flat plate was filled and sanded to make a flush connection. With the total built-up thickness for the plate of 2.21 cm, the 6:1 leading edge was 6.63 cm in length. A photograph of the flat-plate with leading edge inside the test section is shown in Figure-2.

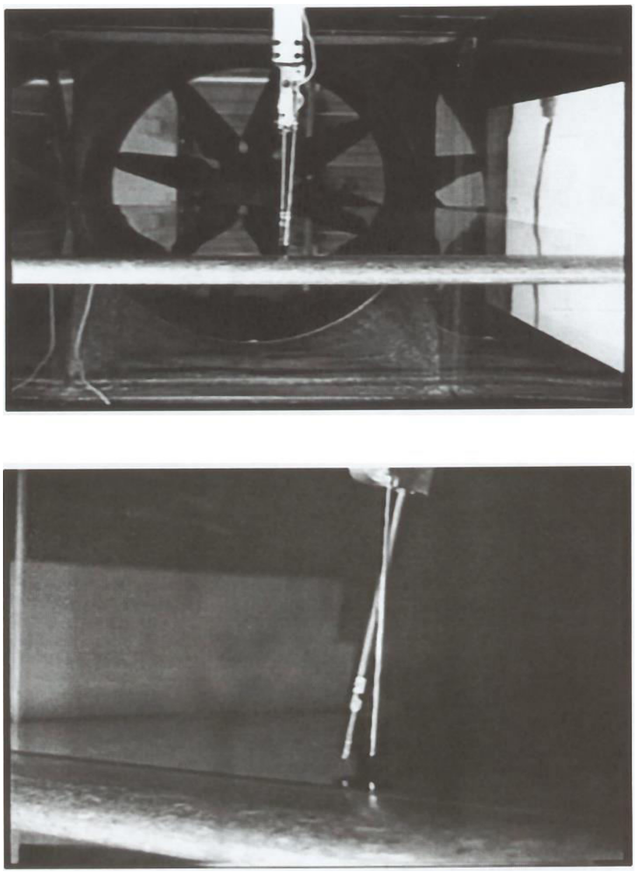

**Figure-2.** Flat plate with a 6:1 elliptic leading edge inside the wind tunnel test section.

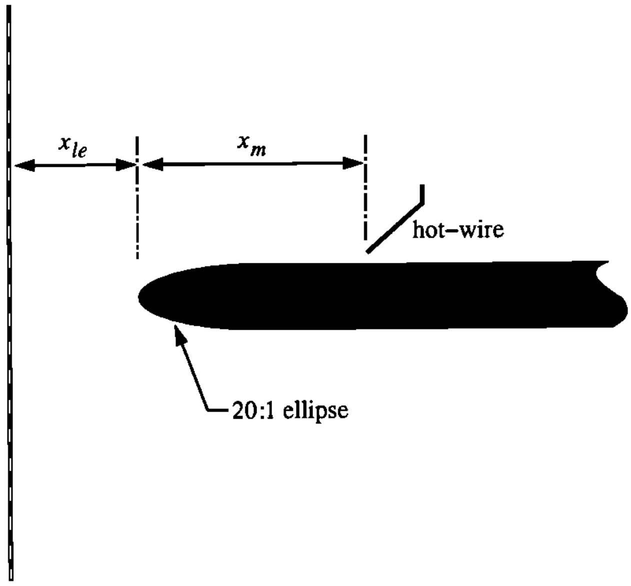


**Figure-3.** Schematic showing the coordinates for measurements.

A schematic of the setup is shown in Figure-3. In this, the distance from the perforated plates to the leading edge is designated $x_{le}$. The measurements were made with a hot-wire held on a traversing mechanism that moved in all three space dimensions. The stream wise distance from the leading edge to the hot-wire is designated $x_m$.

## 3. RESULTS

Hot-wire measurements were taken at different downstream locations in order to establish the turbulence levels and decay rates for the three perforated grids. The results are plotted in Figure-4. In this plot, the downstream distance is normalized by the mesh length, $M$. The total r.m.s. of stream wise velocity fluctuations, u', is represented as the $(U_\infty/u')^2 \times 10^{-2}$, which is the traditional method for indicating the stream wise $u'$ decay with distance from the grid. The different symbols indicate the different perforated grids. The larger mesh grids (PP#2 and PP#3) show a relatively linear decay (constant decay rate) with distance. There also exists a region of overlap where different physical distances ($x$) produce the same $u'$ levels. The smallest mesh grid (PP#1) demonstrates a slower (almost $\sqrt{x}$) decay. This however has a range where the $u'$ fluctuations are comparable to the larger mesh grid, PP#3, so that for the same turbulence levels, the effect of the turbulence scales can be examined.

VOL. 13, NO. 24, DECEMBER 2018 ISSN 1819-6608
ARPN Journal of Engineering and Applied Sciences

www.arpnjournals.com

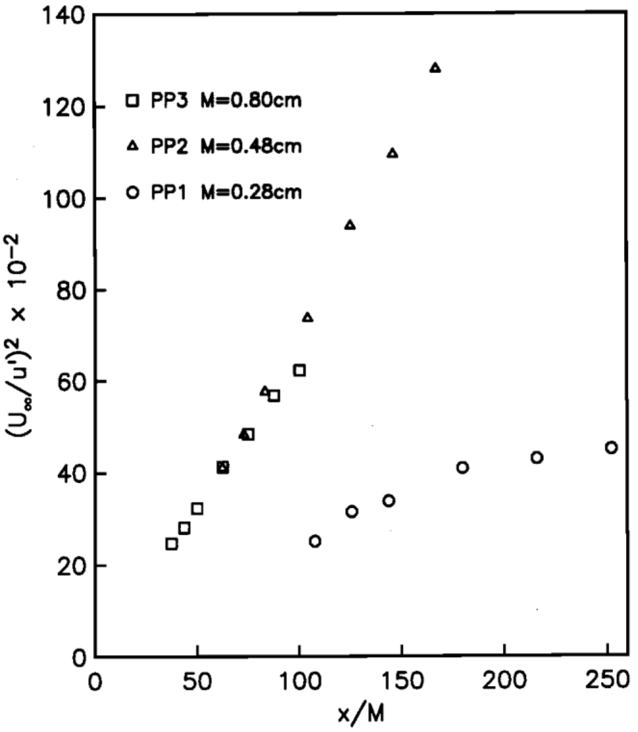


**Figure-4.** Stream wise velocity fluctuation levels downstream of different perforated grids.

An example of the spectrum of stream wise velocity fluctuations for the most up-stream physical location ($x$=29.85 cm, $x/M$ = 37.5) is shown in Figure-5. Indicated on the plot are the -5/3 and -7/3 slopes corresponding to the inertial and viscous sub-ranges for free-stream turbulence, respectively. This spectrum is fairly typical of all the three grids. As the turbulence developed further downstream, a more well defined inertial sub-range was found to develop.

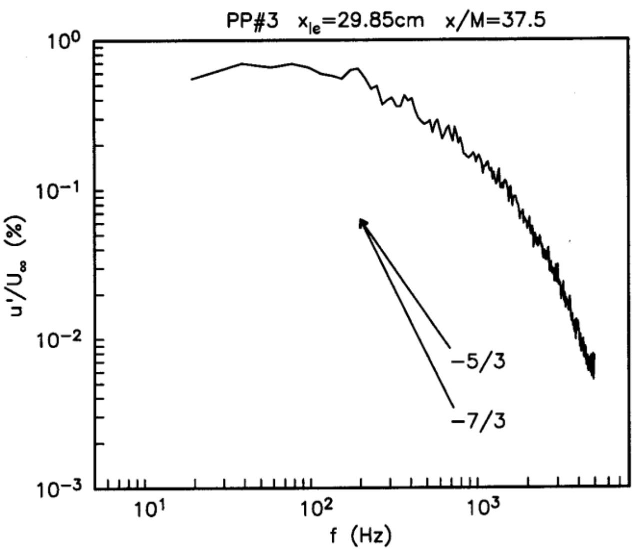


**Figure-5.** Spectrum of streamwise velocity fluctuations for PP#3 at $x$=29.85cm or $x/M$=37.5.

The turbulence produced by the grids represented the unsteady initial condition for the boundary layer flow over the leading edge of a flat plate. The experiment was designed so that the distance from the flat plate to the leading edge could be varied so that the local turbulence level could be varied according to Figure-4.

The measurements were taken at a free-stream speed of 8.5m/s. This was comparable to the velocity used by Kendall (1985, 1990) [2, 3], so that direct comparisons could be made. The measurements consisted of traversing a hot-wire in the wall-normal direction at a particular streamwise/spanwise ($x$,$z$) coordinate. The initial distance of the sensor from the wall was set by the point where electronic contact was made by a conducting probe on the metal wall. The wall contact probe is to the right of the hot-wire in the photographs in Figure-2. Contact was sensed by the data acquisition computer, as a drop in the voltage potential on the contact probe, which was connected to one bit of a digital parallel input.

The hot-wire was operated in a constant temperature mode using a TSI IFA-300 anemometer. The anemometer output was calibrated against known velocities and fit using a 4$^{th}$-order polynomial. All of the voltage time series were pre-processed using analog circuits to d.c.-bias and amplify the signals to minimize quantization error, and anti-alias filtered before acquiring them in an A/D-converter in the data acquisition computer. For documenting the free-stream turbulence generated by the grids, the time series were digitally acquired at 16kHz.

A total of 256 records having 512 contiguous points, were sampled to obtain smooth averaged spectra. For the measurements in the boundary layer, the primary interest is the Klebanoff mode [1], which is quasi-steady. Therefore a slower acquisition rate of 500Hz was used. For this, 32 records of 512 points each were sampled.

Figures 6 and 7 show a sample of the results for the three perforated grids. In these figures, the distance from the grid to the leading edge was kept fixed at $x_{le}$ = 29.85cm. Measurements in the boundary layer were taken at different locations downstream of the leading edge, and in the span wise direction. These were analysed in terms of the wall-normal profiles of the mean velocity and total r.m.s. of stream wise fluctuations. Samples of these profiles are shown in Figure-6. These show the mean and r.m.s. velocities normalized by the free-stream speed ($U_\infty$). The $y$-coordinate is shown in physical dimensions (mm).

VOL. 13, NO. 24, DECEMBER 2018 ISSN 1819-6608
ARPN Journal of Engineering and Applied Sciences

www.arpnjournals.com

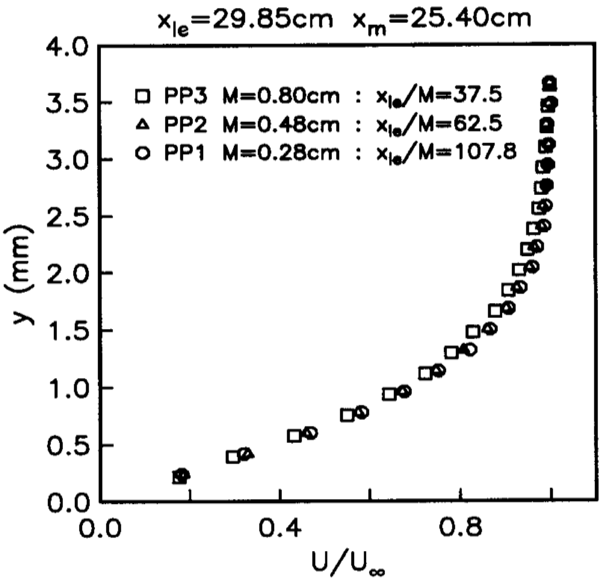


**Figure-6.** Mean velocity profiles at $x_m$=24.4cm for the three perforated grids with $x_{le}$=29.85cm.

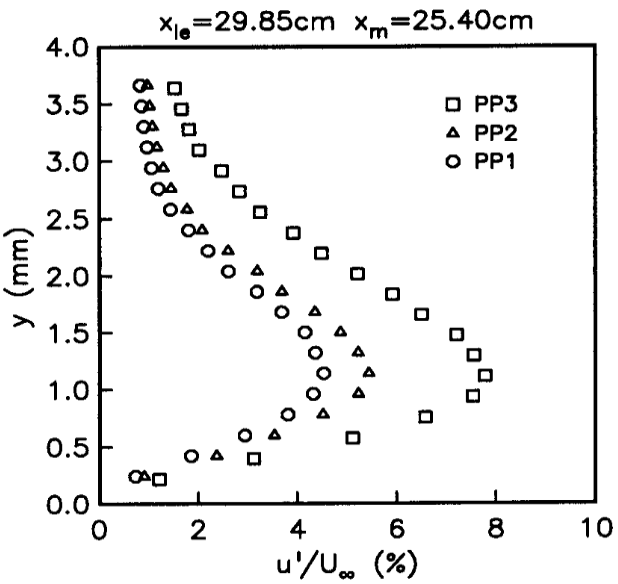


**Figure-7.**The r.m.s. velocity profiles at $x_m$ = 24.4cm for the three perforated grids with $x_{le}$ = 29.85cm.

In these Figures 6 and 7, the profiles are plotted in different symbols which reflect the three perforated grids used. The free-stream turbulence level varies for the three grids, with the largest corresponding to PP#3, and then decreasing through PP#2 and PP#1. The *u'* distribution through the boundary layer shows a smooth variation with a single peak. The location of the peak is independent of the three grid cases. This distribution is the same as those obtained by Kendall (1985, 1990, 1993) [2,3,5] and is associated with the Klebanoff mode (Klebanoff & Tidstrom, 1959 [1]). The fluctuations which make up the total r.m.s. in this case are primarily low frequency. The streamwise location of the measurements is upstream of amplified T-S waves, so that these do not contribute to the *u'* distribution. The mean velocity profiles in these cases are fairly similar, except for a possibly slightly thicker boundary layer in the highest disturbance condition.

We then check if the peak values of *u'* profiles given in Figure-7 correlates with the free-stream disturbance level. This is verified in Figure-8.

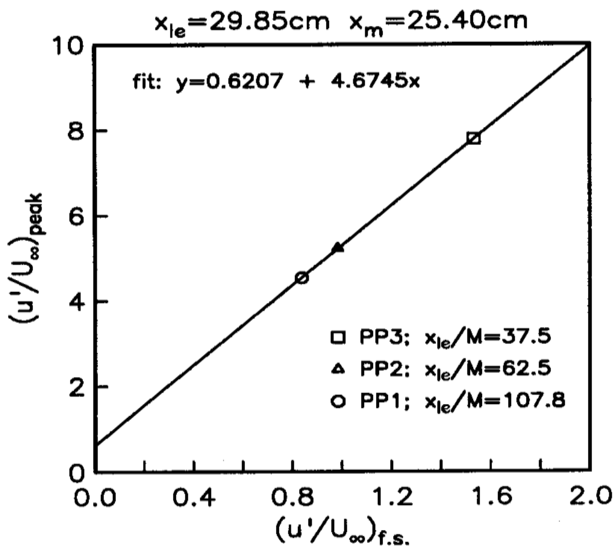


**Figure-8.** Relation between the peak values in the boundary layer to free-stream values at the same x location.

In Figure-8 the peak *u'* values are plotted against the free-stream levels for the three perforated grid cases. These are seen to fall on a linear curve. The formula obtained by a linear fit is given below

$$(u'/U_\infty)_{peak} = 0.6207 + 4.6745\ (u'/U_\infty)_{free\text{-}stream} \quad (1)$$

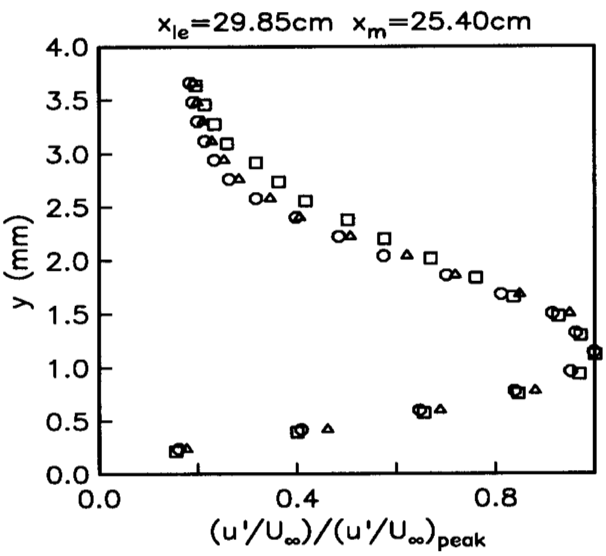


**Figure-9.** The r.m.s. velocity profiles in the boundary layer normalized by the peak values for the three perforated grids.

When the peak values are used to normalize the u' profiles, there is a fairly good collapse of the three perforated grid cases, as seen in Figure-9. This suggests a self-similar nature which is important if the measurements are not made at the peak amplitude location, but rather at some other location in the boundary layer.

The fact that the input/output relation in equation (1) does not pass through zero is interesting. The possible reason for this is that the free-stream value of $u'/U_\infty$ used in the figure 8 and the linear fit was made to the values at the edge of the boundary layer, which is downstream of the leading edge. As indicated in Figure-4, the $u'$ level upstream at the location of the leading edge, will be larger in each case. Therefore the Figure 8 was re-plotted in Figure-10 using the $u'/U_\infty$ values at the $x$-location of the leading edge to represent the disturbance input in each case. For this, only perforated gridsPP#2 and PP#3 were used. The reason for this is that the $u'$ values in the free-stream at the downstream location where the profiles were taken with PP#1 were considerably different than what was previously presented in Figure-4. This prevented us from extrapolating to the leading-edge value with any confidence.

In Figure-10, the points for PP#2 and PP#3 are shown, along with a dashed line which represents a linear fit through the points. The equation of the fit is given in the upper part of the figure. For reference, the solid curve is the fit obtained in Figure-8. The slope of the line, which is based on the leading-edge values, is relatively close to that obtained using the downstream free-stream values. The offset is however different, as expected.

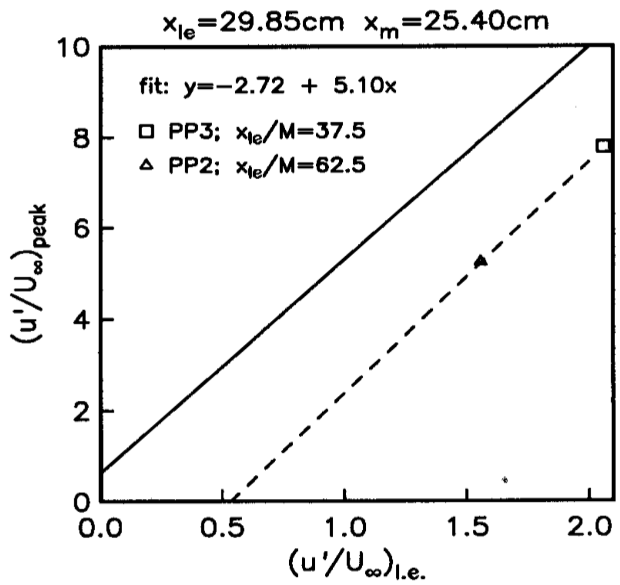


**Figure-10.** Relation between the peak $u'$ values in the boundary layer to free-stream values at the leading edge.

## 4. CONCLUSIONS

Wind tunnel experiments are performed in an attempt to correlate the fluctuation magnitudes in the boundary layer to the fluctuation magnitude in the free-stream. This will allow indirect measurement of the free-stream turbulence levels by measuring the fluctuations in the boundary layer and this indirect measurement is suitable for adverse conditions that exist in cryogenic wind tunnels where direct hot wire measurements are not possible. The measured r.m.s. velocity distributions in the boundary layer agreed well with those associated with the Klebanoff mode. Our results show that there is a linear relation between the magnitude of the Klebanoff mode and the free-stream turbulence level.

## REFERENCES

[1] Klebanoff PS, Tidstrom KD. 1959. Evaluation of amplified waves leading to transition in a boundary layer with zero pressure gradient. NASA TN D-195.

[2] Kendall JM. 1985. Experimental study of disturbances produced in a pretransitional laminar boundary layer by weak free-stream disturbances. AIAA 85-1695.

[3] Kendall JM. 1990. Boundary layer receptivity to free-stream turbulence. AIAA 90-1504.

[4] Loehrke R, Nagib H. 1972. Experiments on management of free-stream Turbulence. AGARD-R-598.

[5] Kendall JM. 1993. Boundary layer receptivity to weak free-stream turbulence. Proceedings of the End-Stage Transition Workshop, University of Syracuse, NY.